Journal of Materials Chemistry C

PAPER

View Article Online
View Journal | View Issue

Cite this: J. Mater. Chem. C, 2015, 3, 1680

Heteroleptic platinum(II) NHC complexes with a C^C* cyclometalated ligand – synthesis, structure and photophysics†

Alexander Tronnier,[a] Ute Heinemeyer,[b] Stefan Metz,[b] Gerhard Wagenblast,[b] Ingo Muenster[b] and Thomas Strassner*[a]

Received 12th November 2014
Accepted 11th December 2014

DOI: 10.1039/c4tc02575j

www.rsc.org/MaterialsC

Platinum(II) complexes [(NHC)Pt(L)] with various β-diketonate based auxiliary ligands (L: 3-meacac = 3-methylacetylacetonato, dpm = dipivaloylmethanato, dbm = dibenzoylmethanato, mesacac = dimesitoylmethanato, duratron = bis(2,3,5,6-tetramethylbenzoyl)methanato) and a C^C* cyclometalated *N*-heterocyclic carbene ligand (NHC: dpbic = 1,3-diphenylbenzo[*d*]imidazol-2-ylidene, dpnac = 1,3-diphenylnaphtho[2,3-*d*]imidazol-2-ylidene or bnbic = 1-phenyl-3-benzylbenzo[*d*]imidazol-2-ylidene) were found to show different aggregation and photophysical properties depending on the auxiliary ligand. Eight complexes were prepared from a silver(I)–NHC intermediate by transmetalation, cyclometalation and subsequent treatment with potassium-*tert*-butanolate and β-diketone. They were fully characterized by standard techniques including ^{195}Pt NMR. Five complexes were additionally characterized by 2D NMR spectroscopy (COSY, HSQC, HMBC and NOESY). Solid-state structures of five complexes could be obtained and show the tendency of the square-planar compounds to form pairs with different Pt–Pt distances depending on the bulkiness of the substituents at the auxiliary ligand. The result of the photophysical measurements in amorphous PMMA films reveals quantum yields of up to 85% with an emission maximum in the blue region and comparatively short decay lifetimes (3.6 μs). Density functional theory (DFT/TD-DFT) calculations were performed to elucidate the emission process and revealed a predominant ^{3}ILCT/^{3}MLCT character. Organic light-emitting devices (OLEDs) comprising one of the complexes achieved 12.6% EQE, 11.9 lm W^{-1} luminous efficacy and 25.2 cd A^{-1} current efficiency with a blue emission maximum at 300 cd m^{-2}. The influence of an additional hole-transporter in the emissive layer was investigated and found to improve the device lifetime by a factor of seven.

Introduction

In the recent past the field of cyclometalated transition metal compounds has received much attention from academia as well as industry. Platinum(II) coordination complexes with their square-planar geometry and numerous potential applications due to their photochemical and photophysical properties are particularly promising. Many contributions in the fields of molecular materials and organic electronics have spurred the research activity of groups worldwide and have proven the versatility of such compounds. Especially their photophysical properties[1] have enabled them to be highly efficient triplet emitters in organic light-emitting devices (OLEDs),[2] chemosensors for oxygen,[3] volatile organics[4] or metal ions,[5] photocatalysts[6] and anticancer agents.[7]

Apart from complexes with tridentate ligands, heteroleptic systems with two bidentate ligands have been investigated as emitters for some time. Prominent motifs in such Pt(II) complexes are monoanionic C^N cyclometalated arylpyridine ligands, which have been tested together with acetylacetonate auxiliary ligands and derivatives thereof.[8] Based on this class of complexes (complex A, Scheme 1) numerous variations regarding substituents,[9] size of the π systems,[10] heterocycles[11]

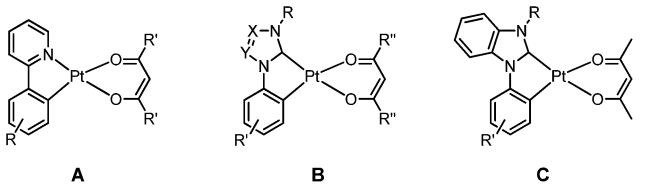

Scheme 1 Examples of cyclometalated Pt(II) complexes.

[a]Physical Organic Chemistry, Technische Universität Dresden, Bergstrasse 66, 01069 Dresden, Germany. E-mail: thomas.strassner@chemie.tu-dresden.de; Fax: +49 351-463-39679; Tel: +49-351-46338571

[b]BASF SE, 67056 Ludwigshafen, Germany

† Electronic supplementary information (ESI) available: Experimental details and characterization data. The CIF files, details of the photophysical measurements, NMR spectra as well as Cartesian coordinates for the optimized structures. CCDC 1011748–1011752. For ESI and crystallographic data in CIF or other electronic format see DOI: 10.1039/c4tc02575j

and auxiliary ligands[12] were studied to tune the photophysical properties.

In combination with *N*-heterocyclic carbene ligands (NHCs) phosphorescent Pt(II) emitters with high quantum yields and blue emission maxima were obtained.[13] When the two concepts of cyclometalation and NHC coordination are merged into one ligand, very stable and efficient emitters are the result. The first compounds of this new class were reported in 2006 (ref. 14) and additional studies were presented since then. Although similar complexes were prepared much earlier,[15] their potential as emitter molecules in OLEDs has only recently been shown.[16] First device tests with a complex of this class showed EQEs as high as 6.2% at 300 cd m^{-2} and a maximum luminance of 6750 cd m^{-2}. Since this discovery, various studies reported examples of this class of C^C* cyclometalated highly emissive complexes (class B, Scheme 1).[17]

The 1,3-diphenylbenzo[*d*]imidazol-2-ylidene (dpbic) has been used as a cyclometalating ligand for iridium(III) emitters before and was recently introduced to platinum(II) (type C, Scheme 1, **1** with R = Ph and R′ = H).[18] Since promising properties like 41% quantum yield, a blue emission (457 nm λ_{max}, CIE: 0.16; 0.15) and a short decay lifetime of 9.2 μs were observed in amorphous PMMA films, we set out to investigate this ligand and derivatives thereof in more detail. Recent studies on the effects of the auxiliary ligand on this novel class of compounds also revealed a significant dependency of the quantum yield, lifetime and aggregation behaviour from the β-diketonate ligand.[19] The influence of five different motifs was analysed at the dpbic system by replacing the common acetylacetonate. Furthermore, the impact of the promising mesacac ligand on a complex with a 1,3-diphenylnaphtho[2,3-*d*]imidazol-2-ylidene ligand (bpnac) and a 1-phenyl-3-benzylbenzo[*d*]-imidazol-2-ylidene ligand (bnbic) is presented.

Results and discussion

Synthesis

Both, dpbic and dpnac were prepared according to literature procedures.[18] 1-Phenylbenzimidazol (**2**) was synthesized by an Ullmann-type coupling reaction with copper(I)oxide and quaternized with benzyl bromide in refluxing THF to give the desired NHC precursor **3**. The synthesis of the auxiliary ligand duratron (**4**) is similar to the one for mesacac. In this protocol durene is reacted with malonyl dichloride in the presence of aluminium(III)chloride in a Friedel–Crafts acylation. All other auxiliary ligands are commercially available.

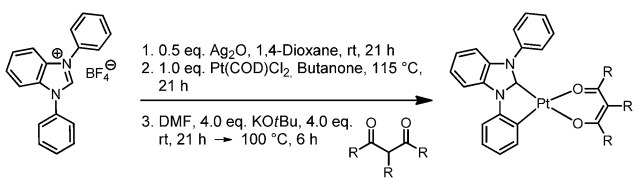

Scheme 2 General synthesis of C^C* cyclometalated complexes.

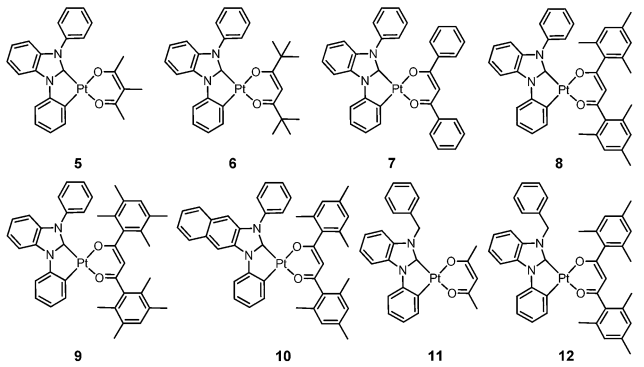

Scheme 3 Synthesized complexes **5–12**.

The Pt(II) complexes **5–12** were prepared in a one-pot synthesis following our established route (**5–9**; Scheme 2): deprotonation of the imidazolium salt with silver(I) oxide in 1,4-dioxane, transmetalation to dichloro(1,5-cyclooctadiene)-platinum(II), cyclometalation at elevated temperature followed by the reaction with the auxiliary ligand in the presence of potassium *tert*-butanolate as a base. The complexes were obtained in yields of 20% to 78% after flash chromatography (Scheme 3).

Characterization

The NMR investigations place the resonance of the ^{13}C carbene carbon signal at 147.4–148.1 ppm in deuterated chloroform as was verified by 2D NMR experiments for **6**, **9**, **10** and **12** (see the ESI, Fig. S1–S8† for examples). This is rather intriguing since some more distinct differences would be expected due to the altered electron density at this site when comparing the mesacac complexes **8**, **10** and **12**. In contrast to this, differences in the signal set can be found for the hydrogen and platinum nuclei. Indeed, in the ^{195}Pt NMR experiments resonances in the typical range for the novel class of C^C* Pt(II) complexes were found between −3298 ppm (**10**) and −3401 ppm (**11**) in $CDCl_3$.

Depending on the auxiliary ligand, the complexes showed quite distinctive solubility in common organic solvents. While all of them were soluble in methylene chloride and chloroform, the compounds with diaryl-substituted diketonates could also be dissolved in less polar halogen free solvents like diethyl ether (**8–10**, **12**) or even isohexanes (**12**).

Melting points for the complexes are as low as 143 °C (**12**) and as high as 275 °C (**6**). Only complex **9** with the duratron ligand **4** shows decomposition (>230 °C). The auxiliary ligand can have a significant effect on the thermal properties, which is palpable for complex **11** with acac ligand (242 °C) compared to complex **12** with the same NHC but the mesacac auxiliary ligand (143 °C). The same holds true for **10** (156 °C) and its acac analogue (285 °C).[18]

Solid-state structure determination

Single-crystals suitable for X-ray diffraction measurements could be obtained for **5–8** (Fig. 1) and **12** (Fig. 2) by slow evaporation of saturated methylene chloride solutions (see ESI,

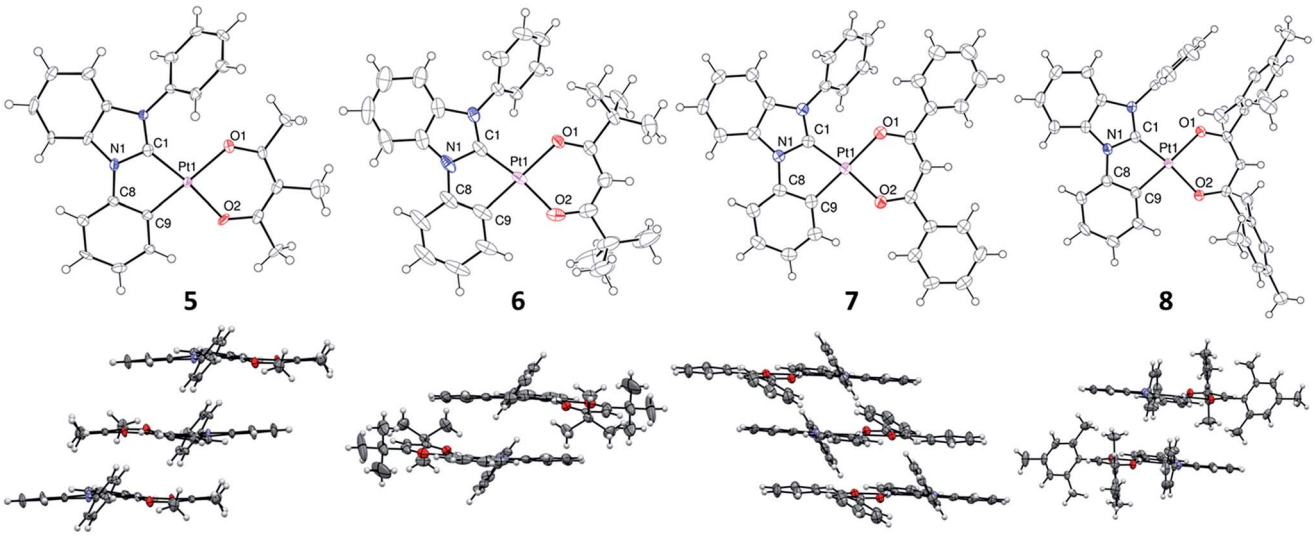

Fig. 1 ORTEP drawing of the solid-state structures of **5–8** and their arrangement in the crystal. Thermal ellipsoids are drawn at 50% probability. The shortest Pt···Pt distances were found to be 3.7845(7) Å (**5**), 6.699(1) Å (**6**), 4.4102(8) Å (**7**) and 5.9509(5) Å (**8**).

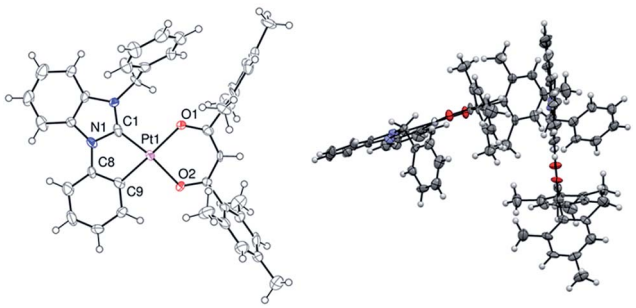

Fig. 2 ORTEP drawing of the solid-state structure of **12** and the molecular arrangement in the crystal. Thermal ellipsoids are drawn at 50% probability.

Tables S1 and S2† for crystal data). The solid-state structures reveal a square-planar coordination of the central Pt(II) atom. The phenyl substituents at the N2 position are always rotated out of the complex plane (dihedral angle 48.4(5)–88.1(4)°), which is comprised of the two metallacycles at the central platinum atom. The angles of these two cycles show some differences regarding the bond angles (Table 1).

While the O1–Pt1–O2 angle shows the nearly perfect 90° for a square-planar coordination (88.1(3)–89.9(3)°), the C1–Pt1–C9 angles are significantly smaller (79.51(16)–80.6(4)°). The four platinum–ligand contacts show some differences as well. While the C1–Pt1 bond is always the shortest (1.923(3)–1.950(12) Å), the platinum–oxygen distances are the longest with O1–Pt1 between 2.070(7)–2.100(2) Å and O2–Pt1 between 2.037(3)–2.062(8) Å. In comparison to the analogous acac complex **1** (Scheme 1),[18] which shows similar values for the four metal–ligand bonds and forms a zigzag structure throughout the crystal with molecule pairs (Pt···Pt distance 6.20 Å), the novel complexes **5–7** are arranged as pairs as well. Compound **8** with the mesacac ligand does not form pairs but uniform layers. By introducing bulky substituents at the auxiliary ligand the Pt···Pt and layer to layer distance increases and thus the tendency to form aggregates decreases. This is important to guarantee monomer emission in the high energy regime when doping amorphous host systems with higher concentrations of emitter (*vide infra*).

Nonetheless, π–π-interactions are observed that are responsible for the layer or pair formation in the solid state. Thus, interlayer separations of 3.62/4.15 Å (**5**), 3.85 Å (**6**), 3.47 Å (**7**) and 5.15 Å (**8**) are found (both metallacycles within a molecule were used for the calculation of a plane). No such direct π–π-interactions could be found for the bulkiest, sterically most demanding complex **12**. For all complex pairs the fashion of the π–π-interaction was found to be similar with the NHC ligand of one complex facing the auxiliary ligand of another (see ESI Fig. S9–S13†).

For complex **12** with the sterically demanding benzyl group and two mesityl groups at the auxiliary ligand, two interwoven layers were found, almost perpendicular to each other (73°). The benzyl group is orientated in such a way, that one hydrogen atom from the methylene moiety forms a H···O1 contact of 2.250(9) Å and the benzyl group is perpendicular to the two coplanar metallacycles.

The presented data from the X-ray diffraction measurements regarding the bond lengths and angles around the metal centre are in good agreement with previously published structures.[17a–d,f,g,20]

Photophysical properties

The photophysical properties of all complexes (**5–12**) were investigated in amorphous poly(methyl methacrylate) (PMMA) films at 2 wt% concentration at room temperature. The films were fabricated with a high enough thickness as to obey the Lambert–Beer law (60–100 nm). Thus, they closely resemble the amorphous environment in a device. We prefer this over

Table 1 Selected bond lengths [Å], angles and dihedral angles [°] of complexes **5–8** and **12**

	5	6	7	8	12
Pt(1)–C(1)	1.947(9)	1.933(4)	1.923(4)	1.923(3)	1.950(12)
Pt(1)–C(9)	1.990(9)	1.991(3)	1.988(5)	1.985(3)	1.983(12)
Pt(1)–O(1)	2.070(7)	2.100(2)	2.088(4)	2.074(2)	2.074(8)
Pt(1)–O(2)	2.037(7)	2.037(3)	2.042(3)	2.041(2)	2.062(8)
C(1)–Pt(1)–C(9)	80.6(4)	79.51(16)	79.90(19)	79.87(13)	79.9(5)
O(1)–Pt(1)–O(2)	88.1(3)	88.79(10)	89.35(13)	89.68(9)	89.9(3)
Pt(1)–C(1)–N(1)–C(8)	3.3(1)	−7.3(4)	−7.4(4)	2.8(4)	0.3(13)

measurements in solution, where solvatochromism can occur. The latter is an important aspect when using different solvents since the triplet properties of transition metal complexes are not independent from the compounds environment[21] and the complexes show significant dipole moments. Previous investigations by our group for the class of C^C* cyclometalated Pt(II) NHC complexes in solution using deaerated methylene chloride or dimethyl sulfoxide and the work of others[22] showed only very weak or even no photoluminescence above the detection limit. Furthermore, during solution experiments in some cases very different properties, like much lower quantum yields, were observed, although the compounds show very similar emission spectra in thin films.[17a,23] For all these reasons we solely focussed on solid-state measurements in this work.

The UV/Vis absorption spectra at 298 K of complexes **5–12** as well as the reference complex **1** [(dpbic)Pt(acac)][18] are depicted in Fig. 3. All nine complexes show weak absorption and similar spectra with an intense absorption band below 270 nm, a smaller shoulder at 300 nm and a second intense band at 310–330 nm (350 nm for **10**). For complex **7** with the dibenzoylmethane (dbm) auxiliary ligand an additional low energy band was found at 380 nm.

The high energy absorptions were assigned to spin allowed $^1\pi$–π^* transitions anticipated for the aromatic heterocycles. These processes are mainly of ILCT character with only small contributions from the diketone auxiliary ligand as indicated by TD-DFT calculations on the fully optimized singlet ground state geometries. The weaker absorptions at lower energy were attributed to metal-to-ligand charge transfers (MLCT), while the stronger absorption around 325 nm showed a HOMO−1 → LUMO configuration for all compounds.

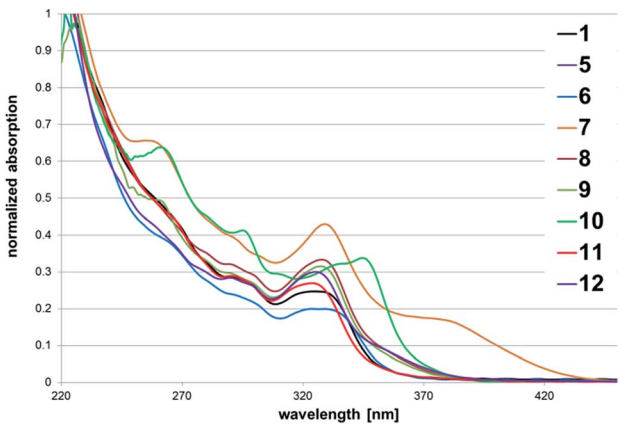

Fig. 3 Absorption spectra of complexes **5–12** and the reference complex **1** [(dpbic)Pt(acac)][18] at room temperature (2 wt% in PMMA).

All of the synthesized complexes show intense phosphorescence at room temperature from the deep blue (454 nm) to the yellow-green (520 nm) region of the visible spectrum (Table 2) with the exception of **5**. For this compound only weak photoluminescence with 4% quantum yield (QY) was observed. This is rather surprising as the only difference is the additional methyl group in the acac backbone in comparison to the reference complex **1** (41% QY).

The emission spectra shown in Fig. 4 display two distinctive types of profiles. For **10** and **11** a well-structured emission profile was observed with maxima at 517 nm (**10**) and 454 nm (**11**) respectively for the electronic transitions and strong vibronic coupling with progression distances of ∼1380–1425 cm^{-1} (**10**) and ∼1220–1275 cm^{-1} (**11**) that correspond well to ground state modes of the NHC ligand as derived from the frequency analysis of the DFT calculations. It is notable that the dpnac NHC ligand with the more extended π-system induces stronger vibronic coupling. These observations already suggest a strong participation of the NHC ligand in the emission process and a significant intraligand charge transfer (^{3}ILCT) character of the triplet manifold. This is in accordance with the measured long decay lifetime (τ_o = 100 μs) of the triplet state of **10**, because of only small ^{3}MLCT contribution.

The profile of complex **6** with the dipivaloylmethanato ligand shows no vibrationally induced bands of this magnitude and is very similar to the spectrum of the reference complex **1** [(dpbic)-Pt(acac)] with a maximum at 460 nm and a hypsochromic weaker shoulder at 440 nm. However, the quantum yield is increased by 13% compared to **1**.

The most notable effect in the spectra was observed when diaryl diketonates were used as the auxiliary ligands. As observed before,[19] dibenzoylmethane as ligand (**7**) lead to a significant bathochromic shift of the emission wavelength, an emission profile with just one broad band, a comparatively high quantum yield (78%) and a short decay lifetime (4.8 μs). DFT calculations show a rotation of the two phenyl groups into the plane of the diketonate core in the triplet state, thus forming a more extended π-system. This in turn allows for an increased delocalization of the lowest π*-orbital of the auxiliary ligand, which as a consequence becomes the LUMO.[2g] In this regard the dbm ligand acts as the new chromophoric unit.

Table 2 Photoluminescence data (2 wt% in PMMA, 100% film in parentheses, room temperature) of cyclometalated complexes **6–12** and the reference complex **1**

#	λ_{exc}/nm[a]	CIE x; y[b]	λ_{em}/nm[c]	Φ[e]	τ_o/μs[f]	$k_r/10^3$ s^{-1}[g]	$k_{nr}/10^3$ s^{-1}[h]
1[i]	340	0.16; 0.15 (*0.34; 0.55*)	457 (*546*)	41 (*31*)	9.2 (*2.8*)	108.4 (*352.3*)	154.7 (*784.1*)
6	355	0.16; 0.16 (*0.19; 0.23*)	461 (*466*) 479[d]	54 (*13*)	7.8 (*6.5*)	127.7 (*154.9*)	107.0 (*1064.6*)
7	375	0.30; 0.56 (*0.43; 0.54*)	520 (*553*) 527[d]	78 (*14*)	4.8 (*5.7*)	208.6 (*175.6*)	58.8 (*1106.4*)
8	330	0.18; 0.26 (*0.23; 0.41*)	473 (*497*) 475[d]	81 (*46*)	4.2 (*3.3*)	238.0 (*302.6*)	56.9 (*351.0*)
9	355	0.17; 0.22 (*0.21; 0.35*)	465 (*486*) 475[d]	81 (*17*)	4.4 (5.2)	226.1 (*194.3*)	51.7 (*942.0*)
10	355	0.31; 0.60 (*0.32; 0.50*)	517 (*523*) 510[d]	82 (*2*)	100.5	9.9	2.2
11	340	0.18; 0.20 (*0.25; 0.49*)	454 (*522*) 443[d]	53 (*43*)	7.3 (*1.0*)	138.0 (*1011.9*)	120.4 (*1369.0*)
12	325	0.18; 0.27 (*0.24; 0.43*)	476 (*497*) 472[d]	85 (*20*)	3.6 (*7.4*)	276.0 (*135.9*)	48.7 (*553.8*)

[a] Excitation wavelength. [b] CIE coordinates at rt. [c] Emission maximum wavelength. [d] Predicted wavelength (see DFT section). [e] Quantum yield in % at λ_{exc}, N_2 atmosphere. [f] Decay lifetimes (excited by laser pulses (355 nm, 1 ns)) given as $\tau_o = \tau_v/\phi$. [g] $k_r = \phi/\tau_v$. [h] $k_{nr} = (1 - \phi)/\tau_v$. [i] [(dpbic)Pt(acac)].[18]

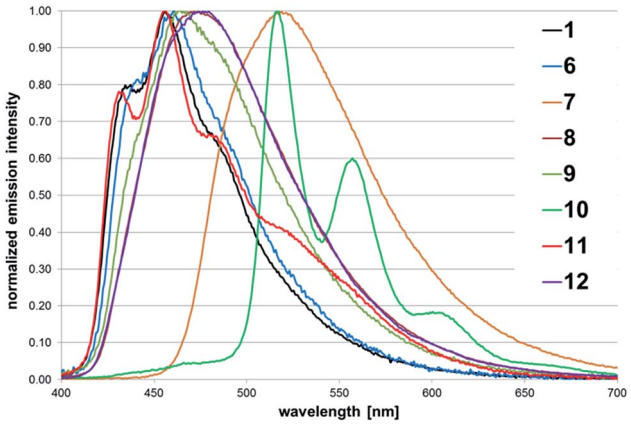

Fig. 4 Emission spectra of complexes **6–12** and the reference complex **1** [(dpbic)Pt(acac)][18] at room temperature (2 wt% in PMMA).

For the other four complexes with aryl substituents at the auxiliary ligand (**8–10** and **12**) such a rotation and subsequent stabilization of the ligands π*-orbital is not possible since the methyl groups in *ortho* position effectively suppress this triplet rearrangement.

Therefore, no significant red-shift was observed. On the other hand, a considerable increase of the quantum yields was achieved with a maximum of 85% for **12**, while for Pt(II) complexes comparatively short decay lifetimes (3.6 μs for **12**) were measured. As for **7**, just one broader emission band is registered for three of these complexes. It is notable that the same effect did not occur with compound **10**. Compared to its acac analogue,[18] the emission maximum, profile and quantum yield of **10** are unchanged. However, the decay lifetime (400 μs with acac) was shortened by a factor of four. When comparing the different methyl-substituted diarylketonates (**8** *vs.* **9**), both seem very similar regarding the QY and decay lifetime. However, for **9**, with the durene substituted auxiliary ligand (**4**), a small hypsochromic shift can be identified. Although small ($\Delta\lambda_{em}$ = 8 nm), this effect can become important when optimizing the resulting colour, charge balance or efficacy of a device.

Furthermore, amorphous, pure emitter films were prepared for **6–12** to probe for concentration dependent effects like excimer formation (see ESI, Fig. S14 and S15†). Indeed, the emission spectra show some distinctive differences. No vibronic coupling was found anymore but for the dpnac complex **10**. Furthermore, all emission maxima are slightly red-shifted (5–33 nm) with the exception of complex **11** and the reference complex C [(dpbic)Pt(acac)] where a significant bathochromic shift of about 70 nm respectively 90 nm was observed (Table 2). Both retain a moderate quantum yield (PMMA → film, 53 → 43% and 41 → 31%) and show very short decay lifetimes (1.0 μs and 2.8 μs) when going from a diluted PMMA to a pure emitter film. Since the two bear acac as auxiliary ligand, no mentionable steric shielding is existent, so that they tend to form aggregated species with short Pt···Pt contacts, thus triggering ^{3}MMLCT processes. The other compounds, with more steric demand induced by the bulky auxiliary ligands, show quantum yields ranging from 2–46% with the greatest drop in efficiency for **10**. As derived from the solid-state structures and DFT calculations no excimer formation should occur for these complexes.

In summary, most of the herein presented auxiliary ligands improve the photophysical properties of the (dpbic)Pt(II)-system and are superior to the common acetylacetonate.

Electroluminescence

Due to its interesting properties like high quantum efficiency, blue phosphorescence and suppressed stacking behaviour, the mesacac functionalized complex **8** was used in the fabrication of blue OLEDs. The device architecture is presented in Fig. 5 and the chemical structures of the device materials are given in the ESI (Fig. S16†). The device setup was chosen for comparison reason with previously reported materials. As a host 2,8-bis-(triphenylsilyl)dibenzo[*b*,*d*]furan (**13**) was selected due to its wide band gap, good morphology characteristics and suitability for the fabrication process.[24] The devices were fabricated by thermally depositing thin layers under high vacuum conditions on an indium tin oxide (ITO) coated glass substrate with a 35 nm spin-coated layer of Plexcore. A 10 nm thick hole-transport layer of Ir(dpbic)$_3$ (**14**) blended with molybdenum oxide was deposited on top of the substrate, followed by a pure Ir(dpbic)$_3$ layer (10 nm) as electron-blocking layer. In the 40 nm thick emission layer the host **13** was mixed with differing ratios of the emitter **8** (5%, 10%, 20% or 30%) and Ir(dpbic)$_3$ (0–30%, >5%

	Al/LiF
ETL	BCP : Cs_2CO_3 (25 nm)
HBL	**13** (5 nm)
EML	**8** : **13** : **14** (40 nm)
HTL	**14** (10 nm)
HIL	**14** : MoO_3 (10 nm)
	ITO
	Glass

Fig. 5 Device layout. **13** = 2,8-bis(triphenylsilyl)dibenzo[*b*,*d*]furan, **14** = [Ir(dpbic)$_3$]. ETL = electron-transport layer, HBL = hole-blocking layer, EML = emission layer, HTL = hole-transport layer, HIL = hole-injection layer. BCP = 2,9-dimethyl-4,7-diphenyl-1,10-phenanthroline.

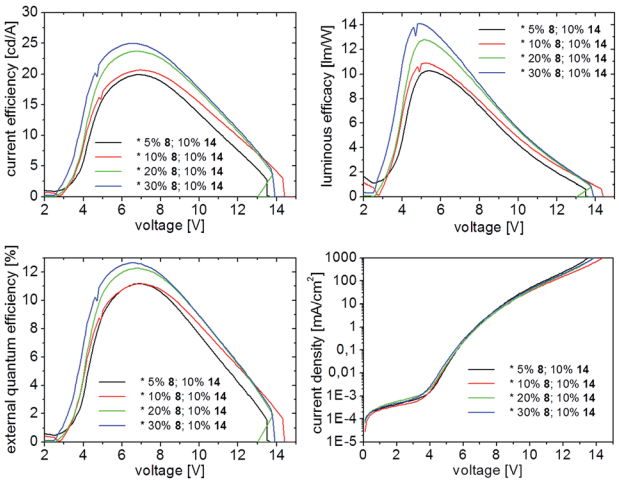

Fig. 6 Mixed-matrix device data at different emitter (**8**) concentrations 5% (black), 10% (red), 20% (green) and 30% (blue) with 10% of **14** plotted against the voltage.

denoted as mixed-matrix device) to facilitate an efficient transport of both holes and electrons and investigate the additives effect on the overall device performance. At last caesium carbonate (5%) blended 2,9-dimethyl-4,7-diphenyl-1,10-phenanthroline (BCP) was deposited as electron-transporting layer, capped with an aluminium electrode.

In the single-matrix OLEDs a continuously increasing performance was observed when the emitter amount was raised from 5% to 30% (see ESI, Fig. S17†). Thus current efficiency of 9.3 cd A^{-1}, luminous efficacy of 2.9 lm W^{-1} and external quantum efficiency (EQE) of 4.6% were achieved at 300 cd m^{-2} (Table 3). Since the operating voltage was rather high, the hole-transporter Ir(dpbic)$_3$ (**14**) was doped in the EML with varying concentrations. The results of the devices with 10% of **14** and different emitter (**8**) concentrations (5% (black), 10% (red), 20% (green) and 30% (blue)) are depicted in Fig. 6. Again, an increased amount of emitter material leads to better performance. It is intriguing that the additional hole-transporter had no significant effect on the charge transporting characteristics as can be derived from the unchanged current density plot, but lowered the operating voltage from over 10 V to 4.8–6.7 V. However, in comparison to the best single-matrix device (10 600 cd m^{-2}) a maximum luminance of 62 750 cd m^{-2} could be generated for a mixed-matrix device with beneficial roll-off properties (Fig. 7). The optimal EML composition was found to be 30% of **8** and 10% of **14**. The corresponding device showed 12.6% EQE, 11.9 lm W^{-1} and 25.2 cd A^{-1} at 300 cd m^{-2}.

Even with an increasing emitter concentration, the emission maximum and colour coordinates were nearly the same like in the 2% PMMA films for the single- as well as the mixed-matrix devices showing good colour purity. Generally, Pt(II) complexes tend to form aggregates due to their square-planar coordination geometry and the possibility of metal–metal interaction through d_z-orbital overlap. When forming aggregated species, no matter if they are excited aggregates, excimers or exciplexes, the Pt(II) compounds show drastically altered photophysical properties.[12d,25] There are many examples in the literature where this is tried to be suppressed by the usage of bulky ligands or substituents. Even units as large as dendrimers were applied to effectively retain monomeric emission properties.[26] In our case the mesityl groups in the periphery of the mesacac auxiliary ligand are sufficient to completely prevent aggregation even at concentrations as high as 30% emitter in the host. This is in agreement with the observations made in the X-ray solid-state experiments, from which the shielding effect of the mesacac ligand could already be guessed.

A critical point in blue emitter research is the operation time of the fabricated devices. The elapsed time before only 50% of the initial luminance of 2000 cd m^{-2} was observed (LT50) was ~1 h and ~7 h for the best single- and mixed-matrix device. Even at 6000 cd m^{-2} LT50 was still over one hour for the latter

Table 3 Device performance with complex **8** at room temperature and 300 cd m^{-2} (doping ratio for **8** : **14**)

Doping [%]	CIE coordinates	Voltage [V]	Cur. eff. [cd A^{-1}]	Lum. eff. [lm W^{-1}]	EQE[a] [%]
5 : 0	0.191; 0.277	11.1	5.91	1.67	3.23
10 : 0	0.193; 0.290	10.9	6.82	1.97	3.61
30 : 0	0.203; 0.322	10.1	9.34	2.91	4.57
30 : 10	0.198; 0.310	6.7	25.20	11.88	12.63
30 : 20	0.194; 0.302	5.4	19.90	11.61	10.20
30 : 30	0.190; 0.289	4.8	16.79	11.01	8.88

[a] External quantum efficiency.

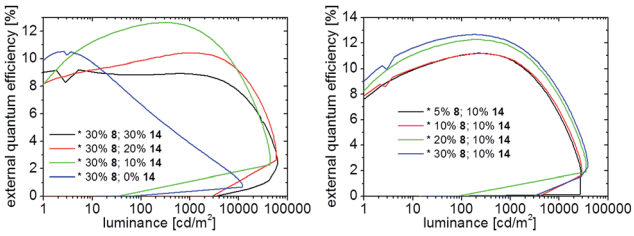

Fig. 7 Mixed-matrix device EQEs for either differing concentrations of **14** and 30% of **8** (left) or differing concentrations of **8** with 10% of **14** plotted against the luminance.

device. Since OLED lifetimes for blue emitters are seldom presented in the literature, it was difficult to compare these values against other cyclometalated platinum(II) systems. In 2013, Li and co-workers presented blue emitter complexes with very high QYs and short decay lifetimes.[2e] However, the lifetimes reported did not exceed one hour at LT50, although the degradation was attributed to the matrix materials and not the emitters.

In comparison to an earlier presented system with a different C^C* cyclometalated NHC and an acac auxiliary ligand that was investigated in the same device architecture,[16] the novel complex **8** presented herein exceeds the former reported parameters (6.2% max. EQE, 6750 cd m^{-2} max. luminance) by far.

DFT calculations

The optimized geometries for the singlet and triplet states have been calculated for all the complexes by DFT methods (B3LYP/6-31G(d) level with a Hay-Wadt-ECP for platinum). The results obtained by these calculations agree well with the structural data gathered from the X-ray diffraction experiments (see ESI, Tables S3–S7†). When changing the multiplicity and moving from the optimized S_0 ground state to the optimized excited T_1 state, significant structural distortions were observed for complexes **5** and **6**. Both compounds show a flipping of the auxiliary diketonate ligand out of the central molecule plane formerly spanned by the two platinacycles. These *pseudo*-Jahn–Teller distortions were the excited system struggles to minimize its energy *via* structural changes are known to lead to fast nonradiative decay.[27]

In the optimized triplet state the two phenyl rings in the diketonate ligand of complex **8** rotate into the plane made up of the metallacycles, thus increasing the conjugation of the π-system as was observed for similar C^C* Pt(II) NHC complexes.[19,28] The corresponding dihedral angles decreased from 28.4° and −28.1° (S_0) to 23.8° and −27.0° (T_1). The resulting stabilisation induced by better delocalisation of the ligands $^3\pi^*$-orbital facilitates the ^{3}LLCT observed in the photophysical experiments. The same did not occur for the other diaryl-substituted complexes. The methyl groups in *ortho* position at the aryl moieties effectively suppress any significant rotations so that the mesityl and durene groups respectively retain their function of shielding the metal centre from interactions, even in the triplet state.

In 2010 Rourke's group investigated the coordination and C^C* cyclometalation of platinum to aryl-benzyl-substituted imidazoles.[29] Only cyclometalation to the benzimidazole bound aryl ring, resulting in the formation of a five-membered metallacycle rather than a six-membered as for benzyl, was observed. In accordance with these results no cyclometalation to the benzyl ring of ligand **3** was observed during our work. If this reaction would occur, the NHC and carbenoid like benzyl fragment would take the positions as in a biscarbene complex. Such a regioisomer to **11** (see ESI, Fig. S18†), with cyclometalation at the benzyl ring (**11iso**), was found to be 6.7 kcal mol^{-1} thermodynamically unfavoured. For the corresponding isomer **12iso** the calculated free energy difference was nearly identical.

On the basis of the optimized S_0 state geometries, the ten first singlet and triplet excitations were calculated by the TD-B3LYP method using the CPCM with dichloromethane as the medium. In Table 4 the calculated vertical excitation energies together with the oscillator strengths, configuration interaction (CI) coefficients, assignments, and the experimental results are summarized. The fitted Gaussian type absorption curves in CH_2Cl_2 are shown in the ESI (Fig. S19–26†).

Since DFT methods have proven to be useful in understanding the photophysical properties of transition-metal complexes,[30] three different methods were employed to ascertain the T_1–S_0 band gap and thus the emission wavelength. The values from the TD-B3LYP calculations all overestimate the gap size by far, while the vertical transition energies obtained using the electronic energy difference between the S_0 and T_1 state at the optimized T_1 geometry are closer to the experimental results although slightly too low. Thirdly, a recently developed method to reliably predict the emission wavelength of transition-metal complexes was used to compute the emission maxima from the vertical transition energies.[31] These values show the best agreement with the ones measured in the experiments.

Frontier Kohn–Sham orbitals as well as spin density surfaces were plotted for all complexes to gain further understanding of the emission properties. They show a significant contribution from the NHC ligand as well as a strong metal d-orbital participation in the highest occupied molecular orbitals (see ESI, Fig. S27 and S28†). These findings underline the character of the charge-transfer states, wherein during the excitation electron density from the central platinum ion as well as the ligands is delocalized to electron-accepting sites of the ligands. This picture of a ^{3}ILCT/MLCT process is supported by the spin density surfaces in Fig. 8. While the diketonate shows only minor contribution for most of the investigated complexes, this does not hold true for **5** and **6**. Here the majority of the density is localized on the auxiliary ligand. From previous investigations we know that this regularly occurs, when the co-ligand flips out of its previous singlet state position.[17f,17g,18] Following Kasha's rule the emission should occur from the lowest excited state. With this in mind the location of the HSOMO, which would be a $^3\pi$-orbital, or rather the ligand on which it is located should strongly influence the photophysical properties. In the photophysical experiments complex **7** with the dbm co-ligand deviates significantly from the other complexes because the

Table 4 Selected triplet excited states (T_n) of **6–12** computed by TD-B3LYP/CPCM (CH_2Cl_2) at the optimized S_0 ground-state geometries

#	T_n	Excitation[a]	Coefficient[b]	Excitation energy[c] (eV)	Character[d]	Vertical transition energy[e] [eV]	Corr. gap[f] [eV]	λ_{em}[g] [nm]	Exp. λ_{em} [nm]
6	T_1	H−1 → L+1	0.44	3.02	^{3}LLCT/^{3}MLCT	2.57	2.59	479	461
	T_2	H → L	0.46	3.05	^{3}IL/^{3}MLCT				
	T_3	H−1 → L	0.54	3.45	^{3}IL/^{3}MLCT				
	T_6	H−2 → L	0.66	3.76	^{3}MLCT				
7	T_1	H−1 → L	0.54	2.60	^{3}LLCT/^{3}MLCT	2.32	2.35	527	520
	T_2	H → L+1	0.57	3.04	^{3}IL/^{3}MLCT				
	T_3	H → L	0.48	3.19	^{3}LLCT/^{3}MLCT				
	T_5	H−1 → L+1	0.53	3.46	^{3}IL/^{3}MLCT				
8	T_1	H−1 → L	0.43	2.89	^{3}IL/^{3}MLCT	2.38	2.61	475	473
	T_2	H → L+1	0.45	3.06	^{3}LLCT/^{3}MLCT				
	T_3	H−1 → L+1	0.46	3.51	^{3}LLCT/^{3}MLCT				
	T_7	H → L	0.40	3.67	^{3}IL/^{3}MLCT				
9	T_1	H−1 → L+1	0.42	2.96	^{3}LLCT/^{3}MLCT	2.38	2.61	475	465
	T_2	H → L	0.52	3.07	^{3}IL/^{3}MLCT				
	T_3	H−1 → L	0.45	3.52	^{3}IL/^{3}MLCT				
10	T_1	H → L	0.53	2.45	^{3}IL/^{3}MLCT	2.13	2.43	510	517
	T_2	H−1 → L+1	0.52	2.91	^{3}LLCT/^{3}MLCT				
	T_4	H−1 → L	0.46	3.31	^{3}IL/^{3}MLCT				
11	T_1	H−1 → L+1	0.46	3.06	^{3}LLCT/^{3}MLCT	2.52	2.80	443	454
	T_2	H → L	0.49	3.09	^{3}IL/^{3}MLCT				
	T_3	H−1 → L	0.47	3.54	^{3}IL/^{3}MLCT				
	T_7	H−2 → L	0.63	3.85	^{3}MLCT				
12	T_1	H−1 → L	0.50	2.89	^{3}IL/^{3}MLCT	2.51	2.63	472	476
	T_2	H → L+1	0.53	3.09	^{3}IL/^{3}MLCT				
	T_4	H−1 → L+1	0.45	3.54	^{3}IL/^{3}MLCT				

[a] Orbitals involved in the major excitation (H = HOMO and L = LUMO). [b] Coefficients in the configuration interaction (CI) expansion. [c] As derived from the TD-DFT calculations using multiple configurations in the single-excitation. [d] Character of the excited state. [e] Obtained by using the electronic-energy difference T_1–S_0 at the optimized triplet geometry (B3LYP/6-31G(d)). [f] Corrected ΔSCF values obtained from BP86 calculations using our wavelength prediction method.[31] [g] Wavelength calculated from the corrected gap values.

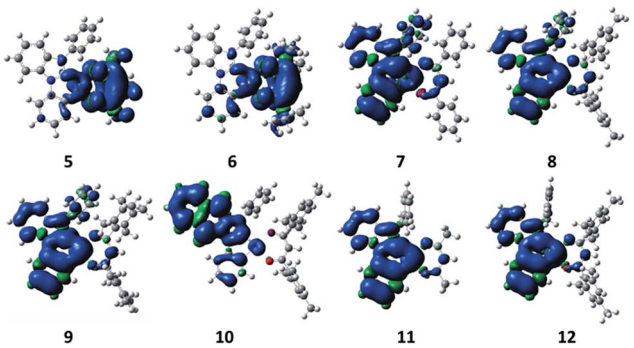

Fig. 8 Spin densities for complexes **5–12** (B3LYP/6-31G(d)).

$^3\pi^*$-acceptor-orbital is localized at the diketonate ligand. Surprisingly, this does not show in the spin density surface.

Conclusions

Eight novel complexes of the class of C^C* cyclometalated Pt(II) complexes with dpbic, dpnac and bnbic as NHC ligands were prepared and investigated. We previously reported on the significant influence from the auxiliary ligand on the physico-chemical and photophysical properties of the resulting C^C* complexes and shed some new light on the right choice of ligands in this work. Thus, highly emissive complexes were designed with emission maxima in the blue region and quantum yields as high as 85% together with a very short decay lifetime of 3.6 μs in 2% PMMA films at room temperature. For the luminophores strong vibronic coupling or one broad emission band was observed depending on the auxiliary ligand, which hints at ILCT/MLCT character of different degree in the triplet manifold. Solid-state structure determinations for five complexes revealed the ability of auxiliary ligands with bulky groups to protect the central metal atom and prevent the square-planar complexes from aggregation. In these cases even pure amorphous emitter films retained good efficiency (QY up to 46%) and showed only minor red-shifts in the emission wavelength. Methyl substituted diaryl diketonate ligands were found to be the best choice as co-ligands in combination with dpbic as NHC ligand because they facilitate good solubility, steric protection and desirable photophysics. This was further demonstrated by one dpnac complex where the previously reported acac analogue showed a decay lifetime over 400 μs. By replacing the acac with mesacac the lifetime is shortened by a factor of 4 with no loss in quantum yield or significant emission red-shift. Furthermore, bnbic was tested as an asymmetric NHC analogue to dpbic together with acac and mesacac as auxiliary ligands. Only cyclometalation to the benzimidazole bound phenyl group was observed which is explained by a thermodynamic preference as verified by DFT calculations. Again, the

comparison of the two compounds reveals the superiority of the mesacac ligand. In contrast, a complex with 3-meacac showed only 4% quantum yield and the choice of dbm led to strongly red-shifted emission, due to a transfer of the LUMO from the NHC to the co-ligand.

Devices prepared with a promising complex achieved 4.6% EQE, 2.9 lm W^{-1} luminous efficacy and 9.3 cd A^{-1} current efficiency at 300 cd m^{-2} with a blue emission color. The performance highly benefitted from the addition of a iridium hole-transporter to the emissive layer and values of 12.6% EQE, 11.9 lm W^{-1} and 25.2 cd A^{-1} at 300 cd m^{-2} were realized. Furthermore, the device lifetime was increased from one to seven hours at 2000 nits. We believe that this rather short lifetime can be attributed to the simplicity and early development stage of the stack design and further improvement is possible by optimization of the device architecture.

Experimental section

General considerations

Solvents of at least 99.5% purity were used throughout this study. 1,4-Dioxane and DMF were dried by using standard techniques and stored under an argon atmosphere over molecular sieves (3 Å). Dichloro(1,5-cyclooctadiene)platinum(II) ($Pt(COD)Cl_2$)[32] was prepared following a modified literature procedure.[16] Dimesitylmethane,[33] (dpbic) and (dpnac) were prepared according to known procedures.[18] All chemicals were obtained from common suppliers and used without further purification. ^1H, ^{13}C and ^{195}Pt NMR spectra were recorded on a Bruker NMR spectrometer. ^1H and ^{13}C NMR spectra were referenced internally by using the resonances of the solvent (^1H: 7.26, ^{13}C: 77.0 for $CDCl_3$; ^1H: 2.50, ^{13}C: 39.43 for DMSO-d_6). ^{195}Pt NMR spectra were referenced externally by using potassium tetrachloroplatinate(II) in D_2O (−1617.2 ($PtCl_4^{2-}$), −2654.1 ($PtCl_2$)). Shifts are given in ppm, coupling constants J in Hz. Elemental analyses were performed by the microanalytical laboratory of our institute on a Hekatech elemental analyser. Melting points have been determined by using a Wagner and Munz Poly Therm A system and are not corrected. The emitter films were prepared by doctor blading a solution of emitter in a 10 wt% PMMA solution in dichloromethane on a substrate with a 60 μm doctor blade.

Synthesis of ligand

1-Phenyl-1*H*-benzo[*d*]imidazole (2). A literature procedure[34] was modified in a way that benzimidazole (1.77 g, 15.0 mmol), iodobenzene (2.04 g, 10.0 mmol), potassium hydroxide (1.12 g, 20.0 mmol) and copper(I) oxide (0.22 g, 1.5 mmol) were suspended in 25 mL of dry DMSO and stirred under argon for 24 h at 120 °C. After cooling, the reaction mixture was poured into 30 mL of water and extracted with 3 × 50 mL of ethyl acetate. The combined organic layers were washed with 50 mL of brine and dried over $MgSO_4$. The crude product was purified by flash chromatography at silica gel with ethyl acetate as eluent. Yield: 1.3 g, 67%. Analytical data are in agreement with the literature. ^1H NMR ($CDCl_3$, 300 MHz): δ 8.14 (s, 1H, NC*H*N), 7.89 (m, 1H, CH_{arom}), 7.52 (m, 6H, CH_{arom}), 7.35 (m, 2H, CH_{arom}) ppm.

3-Benzyl-1-phenyl-1*H*-benzo[*d*]imidazolium bromide (3). The benzimidazole **2** (2.33 g, 12.0 mmol) was stirred with benzyl bromide (6.16 g, 4.3 mL, 36.0 mmol) in 12 mL of THF in a pressure tube for 24 h at 110 °C. After cooling to room temperature, the crude product was precipitated with diethyl ether, collected and washed with diethyl ether in a sonication bath to give an off-white solid after drying in vacuum. Yield: 4.3 g, 99%. ^1H NMR (300 MHz, DMSO-d_6): δ 10.43 (s, 1H, NC*H*N), 8.08–7.99 (m, 1H, CH_{arom}), 7.93–7.83 (m, 3H, CH_{arom}), 7.82–7.69 (m, 5H, CH_{arom}), 7.65 (dd, J = 1.5 Hz, J = 7.9 Hz, 2H, CH_{arom}), 7.48–7.34 (m, 3H, CH_{arom}), 5.87 (s, 2H, CH_2) ppm. ^{13}C NMR (75 MHz, DMSO-d_6): δ 142.8 (N*C*HN), 133.6 (C_i), 133.1 (C_i), 131.3 (C_i), 130.8 (C_i), 130.4 (*C*H$_{arom}$), 130.3 (*C*H$_{arom}$), 128.8 (*C*H$_{arom}$), 128.7 (*C*H$_{arom}$), 128.4 (*C*H$_{arom}$), 127.4 (*C*H$_{arom}$), 127.0 (*C*H$_{arom}$), 125.2 (*C*H$_{arom}$), 114.1 (*C*H$_{arom}$), 113.6 (*C*H$_{arom}$), 50.2 (*C*H$_2$) ppm. M.p.: 199–200 °C. Anal. calcd for $C_{20}H_{17}BrN_2$: C 65.76, H 4.69, N 7.67; found: C 65.76, H 4.68, N 7.63%.

1,3-Bis(2,3,5,6-tetramethylphenyl)propan-1,3-dione (duratron) (4). Malonyl dichloride (29.1 g, 20.0 mL, 200.0 mmol) was added drop wise to a suspension of 1,2,4,5-tetramethylbenzene (132.0 g, 157.0 mL, 980.0 mmol) and dry aluminium chloride (141.0 g, 1060.0 mmol) in 500 mL of carbon disulphide at 0 °C. The mixture was stirred for 72 h at room temperature before it was carefully poured on 300 g of ice and 50 mL of hydrochloric acid (beware: highly exothermic!). After the ice has melted, the two phases were separated, the organic phase washed with water (3 × 200 mL) and evaporated to dryness. The obtained solid was dissolved in 250 mL of chloroform and after the addition of 150 mL of concentrated hydrochloric acid the solution was heated to reflux for 72 h. Afterwards, the cooled phases were separated and the organic phase evaporated to dryness to obtain the product. Yield: 18.8 g, 28%. ^1H NMR (300 MHz, $CDCl_3$): δ 16.03 (s, 1H, O*H*), 6.99 (s, 2H, CH_{arom}), 5.74 (s, 1H, C*H*), 2.22 (s, 24H, CH_3) ppm. ^{13}C NMR (75 MHz, $CDCl_3$): δ 192.4 (*C*O), 137.9 (C_i), 134.1 (C_i), 132.1 (*C*H$_{arom}$), 129.9 (C_i), 105.8 (*C*H), 19.7 (*C*H$_3$), 16.2 (*C*H$_3$) ppm. M.p.: 144–146 °C. Anal. calcd for $C_{23}H_{28}O_2$: C 82.10, H 8.39; found: C 82.45, H 8.05%.

Syntheses of complexes

The established synthetic route for the general synthesis of the platinum(II) complexes **5–12** used silver(I) oxide (93 mg, 0.4 mmol) and NHC ligand precursor (0.8 mmol) in 20 mL of dry 1,4-dioxane at room temperature under argon. $Pt(COD)Cl_2$ (299 mg, 0.8 mmol) and 10 mL of 2-butanone were added to the reaction mixture. The mixture was then refluxed for 21 h and all volatile compounds removed *in vacuo*. Afterwards, 3.2 mmol of the corresponding auxiliary ligand, potassium *tert*-butanolate (357 mg, 3.2 mmol), and 20 mL of DMF were added to the crude reaction mixture. In the last reaction step the solution was stirred for 21 h at room temperature and 6 h at 100 °C. Upon completion all volatiles were removed *in vacuo* again, the remaining solid washed with water, dried and the complexes isolated by flash chromatography with methylene chloride/isohexane (5–3/1) as the eluent.

(SP-4-4)-[3-Methylacetylacetonato][1,3-diphenyl-1*H*-benzo-[*d*]-imidazol-2-ylidene-κC2,κC2′]platinum(II) (5). The synthesis followed the general procedure. 0.39 mL of 3-methylacetylacetone were used. Yield: 93 mg, 20.1%. ^{1}H NMR (300 MHz, $CDCl_3$): δ 8.03 (d, J = 8.1 Hz, 1H, CH_{arom}), 7.93 (dd, J = 1.5 Hz, J = 7.5 Hz, 1H, CH_{arom}), 7.68–7.51 (m, 6H, CH_{arom}), 7.45–7.36 (m, 1H, CH_{arom}), 7.30–7.23 (m, 1H, CH_{arom}), 7.18 (dt, J = 1.5 Hz, J = 7.5 Hz, 1H, CH_{arom}), 7.14–7.09 (m, 1H, CH_{arom}), 7.09–7.03 (m, 1H, CH_{arom}), 2.13 (s, 3H, CH_3), 1.85 (s, 3H, CH_3), 1.38 (s, 3H, CH_3) ppm. ^{13}C NMR (75 MHz, $CDCl_3$): δ 184.3 (*C*O), 182.2 (*C*O), 162.3 (C_i), 148.1 (C_i), 136.5 (C_i), 136.3 (C_i), 131.5 (*C*H$_{arom}$), 131.1 (C_i), 129.3 (*C*H$_{arom}$), 129.1 (*C*H$_{arom}$), 128.4 (*C*H$_{arom}$), 126.8 (C_i), 124.4 (*C*H$_{arom}$), 123.7 (*C*H$_{arom}$), 123.6 (*C*H$_{arom}$), 123.0 (*C*H$_{arom}$), 111.7 (*C*H$_{arom}$), 111.5 (*C*H$_{arom}$), 110.9 (*C*H$_{arom}$), 105.2 (C_i), 27.8 (*C*H$_3$), 27.1 (*C*H$_3$), 16.2 (*C*H$_3$) ppm. ^{195}Pt NMR (64 MHz, $CDCl_3$): δ −3351 ppm. M.p.: 211–213 °C. Anal. calcd for $C_{25}H_{22}N_2O_2Pt$: C 51.99, H 3.84, N 4.85; found: C 52.11, H 3.80, N 4.93%.

(SP-4-4)-[1,3-diphenyl-1*H*-benzo[*d*]imidazol-2-ylidene-κC2,κC2′]-[dipivaloylmethanato]platinum(II) (6). The synthesis followed the general procedure. 602 mg (0.68 mL) of dipivaloylmethane were used. Yield: 210 mg, 40.5%. ^{1}H NMR (300 MHz, $CDCl_3$): δ 8.05 (m, 2H, CH_{arom}), 7.69 (m, 2H, CH_{arom}), 7.60 (m, 3H, CH_{arom}), 7.51 (m, 1H, CH_{arom}), 7.40 (m, 1H, CH_{arom}), 7.23 (d, J = 7.3 Hz, 1H, CH_{arom}), 7.19 (dt, J = 1.9 Hz, J = 7.6 Hz, 1H, CH_{arom}), 7.10 (dt, J = 1.2 Hz, J = 7.4 Hz, 1H, CH_{arom}), 7.05 (d, J = 8.1 Hz, 1H, CH_{arom}), 5.70 (s, 1H, C*H*), 1.27 (s, 9H, CH_3), 0.69 (s, 9H, CH_3) ppm. ^{13}C NMR (75 MHz, $CDCl_3$): δ 195.7 (*C*O), 193.6 (*C*O), 147.9 (C_i), 136.8 (C_i), 136.6 (C_i), 131.5 (*C*H$_{arom}$), 131.0 (C_i), 129.9 (*C*H$_{arom}$), 129.3 (*C*H$_{arom}$), 128.0 (*C*H$_{arom}$), 126.5 (C_i), 124.6 (*C*H$_{arom}$), 123.7 (*C*H$_{arom}$), 123.6 (*C*H$_{arom}$), 123.1 (*C*H$_{arom}$), 111.7 (2 × *C*H$_{arom}$), 110.9 (*C*H$_{arom}$), 92.3 (*C*H), 41.4 (*C*CH$_3$), 41.0 (*C*CH$_3$), 28.7 (*C*H$_3$), 28.0 (*C*H$_3$) ppm. ^{195}Pt NMR (64 MHz, $CDCl_3$): δ −3335 ppm. M.p.: 271–275 °C. Anal. calcd for $C_{30}H_{32}N_2O_2Pt$: C 55.63, H 4.98, N 4.33; found: C 55.82, H 4.86, N 4.19%.

(SP-4-4)-[dibenzoylmethanato][1,3-diphenyl-1*H*-benzo[*d*]-imidazol-2-ylidene-κC2,κC2′]platinum(II) (7). The synthesis followed the general procedure. 732 mg of 1,3-diphenylpropan-1,3-dione were used. Yield: 220 mg, 40.0%. ^{1}H NMR (300 MHz, $CDCl_3$): δ 8.15 (dd, *pseudo*-t, J = 1.6 Hz, J = 7.2 Hz, $J_{H,Pt}$ = 26.1 Hz, 1H, CH_{arom}), 8.10 (dd, J = 1.4 Hz, J = 8.0 Hz, 2H, CH_{arom}), 8.05 (d, J = 8.2 Hz, 1H, CH_{arom}), 7.73 (d, J = 7.9 Hz, 2H, CH_{arom}), 7.64 (d, J = 7.6 Hz, 1H, CH_{arom}), 7.46 (m, 8H, CH_{arom}), 7.17 (m, 8H, CH_{arom}), 6.66 (s, 1H, C*H*) ppm. ^{13}C NMR (75 MHz, $CDCl_3$): δ 180.4 (*C*O), 178.9 (*C*O), 160.7 (C_i), 148.0 (C_i), 139.9 (C_i), 136.5 (C_i), 136.2 (C_i), 131.6 (*C*H$_{arom}$), 131.1 (*C*H$_{arom}$), 130.7 (*C*H$_{arom}$), 130.3 (*C*H$_{arom}$), 129.5 (*C*H$_{arom}$), 129.4 (*C*H$_{arom}$), 128.5 (*C*H$_{arom}$), 128.0 (*C*H$_{arom}$), 127.8 (*C*H$_{arom}$), 127.2 (*C*H$_{arom}$), 127.2 (*C*H$_{arom}$), 125.9 (C_i), 124.7 (*C*H$_{arom}$), 124.0 (*C*H$_{arom}$), 123.9 (*C*H$_{arom}$), 123.2 (*C*H$_{arom}$), 112.0 (*C*H$_{arom}$), 111.7 (*C*H$_{arom}$), 111.0 (*C*H$_{arom}$), 96.8 (*C*H) ppm. ^{195}Pt NMR (64 MHz, $CDCl_3$): δ −3323 ppm. M.p.: 234–236 °C. Anal. calcd for $C_{34}H_{24}N_2O_2Pt$: C 59.39, H 3.52, N 4.07; found: C 59.30, H 3.26, N 4.07%.

(SP-4-4)-[dimesitoylmethanato][1,3-diphenyl-1*H*-benzo[*d*]-imidazol-2-ylidene-κC2,κC2′]platinum(II) (8). The synthesis followed the general procedure. 987 mg of dimesitoylmethane were used. Yield: 256 mg, 41.5%. ^{1}H NMR (600 MHz, DMSO-d_6): δ 8.38 (d, J = 8.3 Hz, 1H, CH_{arom}), 7.84 (d, J = 7.3 Hz, 1H, CH_{arom}), 7.52 (dt, J = 1.3 Hz, J = 7.5 Hz, 1H, CH_{arom}), 7.48 (dd, J = 1.0 Hz, J = 8.3 Hz, 3H, CH_{arom}), 7.36 (t, J = 7.8 Hz, 1H, CH_{arom}), 7.15 (dt, J = 1.4 Hz, J = 7.7 Hz, 1H, CH_{arom}), 7.06 (d, J = 8.1 Hz, 1H, CH_{arom}), 7.01 (t, J = 7.9 Hz, 2H, CH_{arom}), 6.95 (dt, J = 0.9 Hz, J = 7.4 Hz, 1H, CH_{arom}), 6.87 (s, 2H, CH_{arom}), 6.78 (s, 2H, CH_{arom}), 6.59 (t, J = 7.5 Hz, 1H, CH_{arom}), 5.34 (s, 1H, C*H*), 2.30 (s, 3H, CH_3), 2.23 (s, 3H, CH_3), 2.21 (s, 6H, CH_3), 1.95 (s, 6H, CH_3) ppm. ^{13}C NMR (150 MHz, DMSO-d_6): δ 185.6 (*C*O), 182.6 (*C*O), 159.6 (C_i), 147.4 (C_i), 138.6 (C_i), 138.5 (C_i), 137.2 (C_i), 136.3 (C_i), 135.9 (C_i), 134.7 (C_i), 133.2 (C_i), 132.2 (C_i), 130.6 (*C*H$_{arom}$), 129.9 (C_i), 128.3 (*C*H$_{arom}$), 128.1 (*C*H$_{arom}$), 128.0 (*C*H$_{arom}$), 127.3 (*C*H$_{arom}$), 127.2 (*C*H$_{arom}$), 126.2 (C_i), 124.8 (*C*H$_{arom}$), 124.0 (*C*H$_{arom}$), 123.8 (*C*H$_{arom}$), 123.4 (*C*H$_{arom}$), 112.2 (*C*H$_{arom}$), 111.5 (*C*H$_{arom}$), 111.3 (*C*H$_{arom}$), 105.6 (*C*H), 20.7 (*C*H$_3$), 20.6 (*C*H$_3$), 19.3 (*C*H$_3$), 18.6 (*C*H$_3$) ppm. ^{195}Pt NMR (64 MHz, DMSO-d_6): δ −3339 ppm. M.p.: 236–238 °C. Anal. calcd for $C_{40}H_{36}N_2O_2Pt$: C 62.25, H 4.70, N 3.63; found: C 62.28, H 4.79, N 3.72%.

(SP-4-4)-[1,3-diphenyl-1*H*-benzo[*d*]imidazol-2-ylidene-κC2,κC2′]-[1,3-(2,3,5,6-tetramethylphenyl)propan-1,3-dionato] platinum(II) (9). The synthesis followed the general procedure but the first step was done at 50 °C instead of room temperature. 1077 mg of 1,3-(2,3,5,6-tetramethylphenyl)propan-1,3-dione (**4**, duratron) were used. Yield: 318 mg, 49.7%. ^{1}H NMR (500 MHz, $CDCl_3$): δ 8.04 (d, J = 8.2 Hz, 1H, CH_{arom}), 7.84 (dd, J = 1.3 Hz, J = 7.3 Hz, 1H, CH_{arom}), 7.60 (d, J = 7.3 Hz, 1H, CH_{arom}), 7.42–7.38 (m, 1H, CH_{arom}), 7.37–7.34 (m, 2H, CH_{arom}), 7.25–7.22 (m, 1H, CH_{arom}), 7.17 (dt, J = 1.3 Hz, J = 7.6 Hz, 1H, CH_{arom}), 7.05 (d, J = 7.9 Hz, 1H, CH_{arom}), 7.02–6.98 (m, 1H, CH_{arom}), 6.94 (s, 1H, CH_{arom}), 6.92–6.88 (m, 3H, CH_{arom}), 6.56 (t, J = 7.6 Hz, 1H, CH_{arom}), 5.50 (s, 1H, C*H*), 2.22 (s, 6H, CH_3), 2.21 (s, 6H, CH_3), 2.20 (s, 6H, CH_3), 1.91 (s, 6H, CH_3) ppm. ^{13}C NMR (125 MHz, $CDCl_3$): δ 186.5 (*C*O), 184.8 (*C*O), 161.0 (C_i), 148.0 (C_i), 142.3 (C_i), 142.2 (C_i), 136.7 (C_i), 135.3 (C_i), 133.6 (C_i), 132.9 (C_i), 132.1 (*C*H$_{arom}$), 131.0 (*C*H$_{arom}$), 130.9 (C_i), 130.1 (*C*H$_{arom}$), 129.8 (C_i), 128.8 (C_i), 128.5 (*C*H$_{arom}$), 127.9 (*C*H$_{arom}$), 127.6 (*C*H$_{arom}$), 125.9 (C_i), 124.4 (*C*H$_{arom}$), 123.9 (*C*H$_{arom}$), 123.9 (*C*H$_{arom}$), 123.1 (*C*H$_{arom}$), 111.8 (*C*H$_{arom}$), 111.7 (*C*H$_{arom}$), 110.9 (*C*H$_{arom}$), 106.7 (*C*H), 19.7 (*C*H$_3$), 19.6 (*C*H$_3$), 16.5 (*C*H$_3$), 15.7 (*C*H$_3$) ppm. ^{195}Pt NMR (64 MHz, $CDCl_3$): δ −3344 ppm. M.p.: dec. >230 °C. Anal. calcd for $C_{42}H_{40}N_2O_2Pt$: C 63.07, H 5.04, N 3.50; found: C 62.97, H 5.08, N 3.49%.

(SP-4-4)-[dimesitoylmethanato][1,3-diphenyl-1*H*-naphtho-[2,3-*d*]imidazol-2-ylidene-κC2,κC2′]platinum(II) (10). The synthesis followed the general procedure although 0.1 mL of triethylamine were added in the first step. 327 mg of dpnac and 987 mg of dimesitoylmethane were used. Yield: 314 mg, 47.8%. ^{1}H NMR (500 MHz, $CDCl_3$): δ 8.43 (s, 1H, CH_{arom}), 8.06 (d, J = 8.2 Hz, 1H, CH_{arom}), 7.88 (dd, J = 1.3 Hz, J = 7.3 Hz, 1H, CH_{arom}), 7.81–7.76 (m, 2H, CH_{arom}), 7.53 (dt, J = 1.3 Hz, J = 8.2 Hz, 1H, CH_{arom}), 7.49–7.44 (m, 3H, CH_{arom}), 7.42 (s, 1H, CH_{arom}), 7.28–7.22 (m, 1H, CH_{arom}), 7.09–7.02 (m, 3H, CH_{arom}), 6.85 (s, 2H, CH_{arom}), 6.76 (s, 2H, CH_{arom}), 6.65 (t, J = 7.6 Hz, 1H, CH_{arom}), 5.53 (s, 1H, C*H*), 2.35 (s, 3H, CH_3), 2.31 (s, 6H, CH_3), 2.29 (s, 3H, CH_3), 2.02 (s, 6H, CH_3) ppm. ^{13}C NMR (125 MHz, $CDCl_3$): δ 185.9 (*C*O), 183.7 (*C*O), 166.1 (C_i), 147.9 (C_i), 139.3 (C_i), 139.0 (C_i), 137.6 (C_i), 136.9 (C_i), 136.7 (C_i), 135.4 (C_i), 134.2 (C_i), 133.1 (C_i),

131.9 (CH_{arom}), 131.0 (C_i), 130.4 (C_i), 129.8 (C_i), 128.8 (CH_{arom}), 128.4 (CH_{arom}), 128.2 (CH_{arom}), 128.1 (CH_{arom}), 127.9 (CH_{arom}), 127.7 (CH_{arom}), 127.4 (CH_{arom}), 125.8 (CH_{arom}), 125.6 (C_i), 125.3 (CH_{arom}), 124.2 (CH_{arom}), 123.8 (CH_{arom}), 111.8 (CH_{arom}), 108.2 (CH_{arom}), 107.3 (CH_{arom}), 106.3 (*C*H), 21.1 (2 × CH_3), 19.9 (CH_3), 19.0 (CH_3) ppm. ^{195}Pt NMR (64 MHz, $CDCl_3$): δ −3298 ppm. M.p.: 156–157 °C. Anal. calcd for $C_{44}H_{38}N_2O_2Pt$: C 64.30, H 4.66, N 3.41; found: C 64.54, H 4.67, N 3.43%.

(SP-4-4)-[acetylacetonato][3-benzyl-1-phenyl-1*H*-benzo[*d*]-imidazol-2-ylidene-κC2,κC2′]platinum(II) (11). The synthesis followed the general procedure. 292 mg of **3** and 0.33 mL of acetylacetone were used. Yield: 360 mg, 77.9%. ^{1}H NMR (300 MHz, $CDCl_3$): δ 7.94 (dd, *pseudo*-t, J = 1.3 Hz, J = 7.4 Hz, $J_{H,Pt}$ = 28.5 Hz, 1H, C*H*$_{arom}$), 7.93 (d, J = 8.1 Hz, 1H, C*H*$_{arom}$), 7.52 (dd, J = 1.1 Hz, J = 7.9 Hz, 1H, C*H*$_{arom}$), 7.49 (d, J = 6.7 Hz, 2H, C*H*$_{arom}$), 7.31 (m, 5H, C*H*$_{arom}$), 7.23 (m, 1H, C*H*$_{arom}$), 7.17 (dt, J = 1.4 Hz, J = 7.5 Hz, 1H, C*H*$_{arom}$), 7.07 (dt, J = 1.4 Hz, J = 7.5 Hz, 1H, C*H*$_{arom}$), 6.11 (s, 2H, C*H*$_2$), 5.50 (s, 1H, C*H*), 2.09 (s, 3H, C*H*$_3$), 1.78 (s, 3H, C*H*$_3$) ppm. ^{13}C NMR (150 MHz, $CDCl_3$): δ 185.5 (*C*O), 185.4 (*C*O), 160.9 (C_i), 148.1 (C_i), 136.1 (C_i), 134.7 (C_i), 131.6 (C_i), 131.3 (CH_{arom}), 128.6 (CH_{arom}), 127.6 (CH_{arom}), 127.5 (CH_{arom}), 125.5 (C_i), 124.2 (CH_{arom}), 123.9 (CH_{arom}), 123.6 (CH_{arom}), 122.8 (CH_{arom}), 111.6 (CH_{arom}), 111.3 (CH_{arom}), 111.0 (CH_{arom}), 102.1 (*C*H), 48.5 (CH_2), 27.9 (CH_3), 27.7 (CH_3) ppm. ^{195}Pt NMR (64 MHz, $CDCl_3$): δ −3401 ppm. M.p.: 241–244 °C. Anal. calcd for $C_{25}H_{22}N_2O_2Pt$: C 51.99, H 3.84, N 4.85; found: C 52.26, H 3.71, N 4.71%.

(SP-4-4)-[3-benzyl-1-phenyl-1*H*-benzo[*d*]imidazol-2-ylidene-κC2,κC2′][dimesitoylmethanato]platinum(II) (12). The synthesis followed the general procedure. 292 mg of **3** and 987 mg of dimesitoylmethane were used. Yield: 399 mg, 63.5%. ^{1}H NMR (600 MHz, $CDCl_3$): δ 7.99 (d, J = 7.9 Hz, 1H, C*H*$_{arom}$), 7.87 (dd, J = 1.3 Hz, J = 7.3 Hz, 1H, C*H*$_{arom}$), 7.56 (dd, J = 0.8 Hz, J = 7.9 Hz, 1H, C*H*$_{arom}$), 7.36 (dt, J = 1.1 Hz, J = 7.7 Hz, 1H, C*H*$_{arom}$), 7.31–7.28 (m, 1H, C*H*$_{arom}$), 7.26–7.23 (m, 1H, C*H*$_{arom}$), 7.18–7.13 (m, 4H, C*H*$_{arom}$), 7.10–7.07 (m, 2H, C*H*$_{arom}$), 6.99 (dt, J = 1.1 Hz, J = 7.5 Hz, 1H, C*H*$_{arom}$), 6.87 (s, 2H, C*H*$_{arom}$), 6.73 (s, 2H, C*H*$_{arom}$), 5.99 (s, 2H, C*H*$_2$), 5.68 (s, 1H, C*H*), 2.36 (s, 6H, C*H*$_3$), 2.31 (s, 3H, C*H*$_3$), 2.27 (s, 3H, C*H*$_3$), 2.06 (s, 6H, C*H*$_3$) ppm. ^{13}C NMR (150 MHz, $CDCl_3$): δ 185.7 (*C*O), 184.8 (*C*O), 160.8 (C_i), 148.1 (C_i), 139.4 (C_i), 139.1 (C_i), 137.7 (C_i), 137.2 (C_i), 136.1 (C_i), 134.9 (C_i), 134.2 (C_i), 133.5 (C_i), 131.8 (CH_{arom}), 131.5 (C_i), 128.4 (CH_{arom}), 128.2 (CH_{arom}), 127.8 (CH_{arom}), 127.2 (CH_{arom}), 126.6 (CH_{arom}), 125.1 (C_i), 124.3 (CH_{arom}), 124.1 (CH_{arom}), 123.7 (CH_{arom}), 123.0 (CH_{arom}), 111.7 (CH_{arom}), 111.4 (CH_{arom}), 111.0 (CH_{arom}), 107.0 (*C*H), 48.1 (CH_2), 21.2 (CH_3), 21.1 (CH_3), 20.0 (CH_3), 19.1 (CH_3) ppm. ^{195}Pt NMR (64 MHz, $CDCl_3$): δ −3358 ppm. M.p.: 141–145 °C. Anal. calcd for $C_{41}H_{38}N_2O_2Pt$: C 62.67, H 4.87, N 3.56; found: C 62.66, H 4.70, N 3.60%.

Computational details

All calculations were performed with the Gaussian09 package.[35] The density functional hybrid model B3LYP[36] and the gradient-corrected density functional BP86 (ref. 37) were used together with the 6-31G(d)[38] basis set. No symmetry or internal coordinate constraints were applied during optimizations. All reported intermediates were verified as true minima by the absence of negative eigenvalues in the vibrational frequency analysis. In all cases, platinum was described by using a decontracted Hay-Wadt(n + 1) ECP and basis set.[39] Approximate free energies were obtained through thermochemical analysis, by using the thermal correction to Gibbs free energy as reported by Gaussian09. This takes into account zero-point effects, thermal enthalpy corrections and entropy. All energies reported in this paper, unless otherwise noted, are Gibbs free energies at standard conditions (T = 298 K, p = 1 atm), using unscaled frequencies. For visualization, GaussView[40] and CYLview[41] were used.

X-ray crystallography

Preliminary examination and data collection were carried out on an area detecting system (Kappa-CCD; Nonius, FR590) using graphite monochromated Mo K_α radiation (λ = 0.71073 Å) with an Oxford Cryosystems cooling system at the window of a sealed fine-focus X-ray tube. The reflections were integrated. Raw data were corrected for Lorentz, polarization, decay and absorption effects. The absorption correction was applied using SADABS.[42] After merging, the independent reflections were used for all calculations. The structure was solved by a combination of direct methods[43] and difference Fourier syntheses.[44] All non-hydrogen atom positions were refined with anisotropic displacement parameters. Hydrogen atoms were placed in ideal positions using the SHELXL riding model. Full-matrix least-squares refinements were carried out by minimizing $\Sigma w(F_o^2 - F_c^2)^2$ with the SHELXL-97 weighting scheme and stopped at shift/err < 0.001. Moreover, extremely diffuse solvent was present in the lattice of **7**, which was treated by the SQUEEZE option integrated in PLATON. Details of the structure determinations are given in the ESI (cif file).† Neutral-atom scattering factors for all atoms and anomalous dispersion corrections for the non-hydrogen atoms were taken from International Tables for Crystallography.[45] All calculations were performed with the programs COLLECT,[46] DIRAX,[47] EVALCCD,[48] SIR92,[43a] SIR97,[43b] SADABS,[42] PLATON[49] and the SHELXL-97 package.[44,50] For the visualization, mercury[51] and ORTEP-III[52] were used.

Device fabrication

For the production of the devices and testing, an ITO substrate used as the anode was first cleaned by commercial detergents for the LCD-Production (Deconex® 20NS and 25ORGAN-ACID®) followed by immersion in a acetone/isopropanole-mixture in an ultrasonic bath. Afterwards the substrate is treated with ozone to remove residues of organic material. This treatment also improves the hole-injection properties of the ITO substrate. Then the hole-injection layer is spin-coated from solution. This is followed by vacuum deposition of the various organic materials with rates of approximately 0.5–5 nm min^{-1} at 10^{-7} to 10^{-9} mbar. Finally a layer of 0.75 nm lithium fluoride and a 100 nm aluminium electrode are deposited. All diodes are sealed with glass in an inert nitrogen atmosphere. For characterisation of the OLEDs

the electroluminescence spectra were measured at various currents and voltages. The *I–V* characteristic was measured in combination with the emitted light.

Acknowledgements

We are grateful to Dr Fuchs (BASF) and Dr Lennartz (BASF) for helpful discussions. We also thank the ZIH for computation time on their high-performance computing facility and the BMBF (FKZ: 13N10477) for funding.

Notes and references

1 (*a*) J. A. G. Williams, *Top. Curr. Chem.*, 2007, **281**, 205; (*b*) J. A. G. Williams, *Chem. Soc. Rev.*, 2009, **38**, 1783; (*c*) P.-T. Chou and Y. Chi, *Chem.–Eur. J.*, 2007, **13**, 380; (*d*) Y. Chi and P.-T. Chou, *Chem. Soc. Rev.*, 2010, **39**, 638; (*e*) A. F. Rausch, H. H. H. Homeier and H. Yersin, *Top. Organomet. Chem.*, 2010, **29**, 193; (*f*) H. Yersin, W. Humbs and J. Strasser, *Top. Curr. Chem.*, 1997, **191**, 153; (*g*) H. Yersin and Editor, *Highly Efficient OLEDs with Phosphorescent Materials*, Wiley-VCH Verlag GmbH & Co. KGaA, 2008; (*h*) V. W.-W. Yam and K. M.-C. Wong, *Chem. Commun.*, 2011, **47**, 11579.

2 (*a*) M. A. Baldo, D. F. O'Brien, Y. You, A. Shoustikov, S. Sibley, M. E. Thompson and S. R. Forrest, *Nature*, 1998, **395**, 151; (*b*) L. Murphy and J. A. G. Williams, *Top. Organomet. Chem.*, 2010, **28**, 75; (*c*) S.-W. Lai and C.-M. Che, *Top. Curr. Chem.*, 2004, **241**, 27; (*d*) H.-F. Xiang, S.-W. Lai, P. T. Lai and C.-M. Che, *Phosphorescent platinum(II) materials for OLED applications*, 2008; (*e*) X.-C. Hang, T. Fleetham, E. Turner, J. Brooks and J. Li, *Angew. Chem., Int. Ed.*, 2013, **52**, 6753; (*f*) K. Li, G. Cheng, C. Ma, X. Guan, W.-M. Kwok, Y. Chen, W. Lu and C.-M. Che, *Chem. Sci.*, 2013, **4**, 2630; (*g*) W. Lu, B.-X. Mi, M. C. W. Chan, Z. Hui, C.-M. Che, N. Zhu and S.-T. Lee, *J. Am. Chem. Soc.*, 2004, **126**, 4958; (*h*) S. C. F. Kui, P. K. Chow, G. Cheng, C.-C. Kwok, C. L. Kwong, K.-H. Low and C.-M. Che, *Chem. Commun.*, 2013, **49**, 1497; (*i*) A. Y.-Y. Tam, D. P.-K. Tsang, M.-Y. Chan, N. Zhu and V. W.-W. Yam, *Chem. Commun.*, 2011, **47**, 3383; (*j*) B. W. D'Andrade, J. Brooks, V. Adamovich, M. E. Thompson and S. R. Forrest, *Adv. Mater.*, 2002, **14**, 1032; (*k*) V. Adamovich, J. Brooks, A. Tamayo, A. M. Alexander, P. I. Djurovich, B. W. D'Andrade, C. Adachi, S. R. Forrest and M. E. Thompson, *New J. Chem.*, 2002, **26**, 1171; (*l*) C. Cebrian, M. Mauro, D. Kourkoulos, P. Mercandelli, D. Hertel, K. Meerholz, C. A. Strassert and L. De Cola, *Adv. Mater.*, 2013, **25**, 437.

3 (*a*) X.-d. Wang, X. Chen, Z.-x. Xie and X.-r. Wang, *Angew. Chem., Int. Ed.*, 2008, **47**, 7450; (*b*) W. Wu, W. Wu, S. Ji, H. Guo and J. Zhao, *Dalton Trans.*, 2011, **40**, 5953.

4 (*a*) M. Kato, A. Omura, A. Toshikawa, S. Kishi and Y. Sugimoto, *Angew. Chem., Int. Ed.*, 2002, **41**, 3183; (*b*) M. L. Muro, C. A. Daws and F. N. Castellano, *Chem. Commun.*, 2008, 6134; (*c*) L. J. Grove, J. M. Rennekamp, H. Jude and W. B. Connick, *J. Am. Chem. Soc.*, 2004, **126**, 1594; (*d*) Y. Kunugi, L. L. Miller, K. R. Mann and M. K. Pomije, *Chem. Mater.*, 1998, **10**, 1487.

5 (*a*) V. Guerchais and J.-L. Fillaut, *Coord. Chem. Rev.*, 2011, **255**, 2448; (*b*) P.-H. Lanoe, J.-L. Fillaut, L. Toupet, J. A. G. Williams, H. Le Bozec and V. Guerchais, *Chem. Commun.*, 2008, 4333; (*c*) P.-H. Lanoe, J.-L. Fillaut, V. Guerchais, H. Le Bozec and J. A. G. Williams, *Eur. J. Inorg. Chem.*, 2011, 1255.

6 (*a*) D. Zhang, L.-Z. Wu, L. Zhou, X. Han, Q.-Z. Yang, L.-P. Zhang and C.-H. Tung, *J. Am. Chem. Soc.*, 2004, **126**, 3440; (*b*) W. B. Connick and H. B. Gray, *J. Am. Chem. Soc.*, 1997, **119**, 11620; (*c*) M. Hissler, J. E. McGarrah, W. B. Connick, D. K. Geiger, S. D. Cummings and R. Eisenberg, *Coord. Chem. Rev.*, 2000, **208**, 115.

7 (*a*) R. W.-Y. Sun, A. L.-F. Chow, X.-H. Li, J. J. Yan, S. S.-Y. Chui and C.-M. Che, *Chem. Sci.*, 2011, **2**, 728; (*b*) R. Wai-Yin Sun, D.-L. Ma, E. L.-M. Wong and C.-M. Che, *Dalton Trans.*, 2007, 4884.

8 J. Brooks, Y. Babayan, S. Lamansky, P. I. Djurovich, I. Tsyba, R. Bau and M. E. Thompson, *Inorg. Chem.*, 2002, **41**, 3055.

9 (*a*) D. Kourkoulos, C. Karakus, D. Hertel, R. Alle, S. Schmeding, J. Hummel, N. Risch, E. Holder and K. Meerholz, *Dalton Trans.*, 2013, **42**, 13612; (*b*) M. D. Perez, P. I. Djurovich, A. Hassan, G. Y. Cheng, T. J. Stewart, K. Aznavour, R. Bau and M. E. Thompson, *Chem. Commun.*, 2009, 4215.

10 (*a*) A. Bossi, A. F. Rausch, M. J. Leitl, R. Czerwieniec, M. T. Whited, P. I. Djurovich, H. Yersin and M. E. Thompson, *Inorg. Chem.*, 2013, **52**, 12403; (*b*) W. Wu, W. Wu, S. Ji, H. Guo and J. Zhao, *Eur. J. Inorg. Chem.*, 2010, 4470.

11 D. N. Kozhevnikov, V. N. Kozhevnikov, M. Z. Shafikov, A. M. Prokhorov, D. W. Bruce and W. J. A. Gareth, *Inorg. Chem.*, 2011, **50**, 3804.

12 (*a*) M. Spencer, A. Santoro, G. R. Freeman, A. Diez, P. R. Murray, J. Torroba, A. C. Whitwood, L. J. Yellowlees, J. A. G. Williams and D. W. Bruce, *Dalton Trans.*, 2012, **41**, 14244; (*b*) S.-B. Ko, J.-S. Lu, Y. Kang and S. Wang, *Organometallics*, 2013, **32**, 599; (*c*) B. A. Blight, S.-B. Ko, J.-S. Lu, L. F. Smith and S. Wang, *Dalton Trans.*, 2013, **42**, 10089; (*d*) T. Shigehiro, S. Yagi, T. Maeda, H. Nakazumi, H. Fujiwara and Y. Sakurai, *J. Phys. Chem. C*, 2013, **117**, 532.

13 (*a*) Y. Unger, A. Zeller, S. Ahrens and T. Strassner, *Chem. Commun.*, 2008, 3263; (*b*) Y. Unger, A. Zeller, M. A. Taige and T. Strassner, *Dalton Trans.*, 2009, 4786.

14 M. Egen, K. Kahle, M. Bold, T. Gessner, C. Lennartz, S. Nord, H.-W. Schmidt, M. Thelakkat, M. Baete, C. Neuber, W. Kowalsky, C. Schildknecht and H.-H. Johannes, WO2006056418A2, 2006.

15 K. Hiraki, M. Onishi, K. Ohnuma and K. Sugino, *J. Organomet. Chem.*, 1981, **216**, 413.

16 Y. Unger, D. Meyer, O. Molt, C. Schildknecht, I. Muenster, G. Wagenblast and T. Strassner, *Angew. Chem., Int. Ed.*, 2010, **49**, 10214.

17 (*a*) Z. M. Hudson, C. Sun, M. G. Helander, Y.-L. Chang, Z.-H. Lu and S. Wang, *J. Am. Chem. Soc.*, 2012, **134**, 13930; (*b*) A. Tronnier, A. Risler, N. Langer, G. Wagenblast,

I. Muenster and T. Strassner, *Organometallics*, 2012, **31**, 7447; (*c*) T. Strassner, Y. Unger, D. Meyer, O. Molt, I. Muenster and G. Wagenblast, *Inorg. Chem. Commun.*, 2013, **30**, 39; (*d*) M. Tenne, S. Metz, I. Muenster, G. Wagenblast and T. Strassner, *Organometallics*, 2013, **32**, 6257; (*e*) A. Tronnier and T. Strassner, *Dalton Trans.*, 2013, **42**, 9847; (*f*) A. Tronnier, S. Metz, G. Wagenblast, I. Muenster and T. Strassner, *Dalton Trans.*, 2014, **43**, 3297; (*g*) A. Tronnier, A. Poethig, E. Herdtweck and T. Strassner, *Organometallics*, 2014, **33**, 898.

18 A. Tronnier, A. Poethig, S. Metz, G. Wagenblast, I. Muenster and T. Strassner, *Inorg. Chem.*, 2014, **53**, 6346.

19 A. Tronnier, N. Nischan, S. Metz, G. Wagenblast, I. Muenster and T. Strassner, *Eur. J. Inorg. Chem.*, 2014, **2014**, 256.

20 (*a*) A. Tronnier and T. Strassner, *Dalton Trans.*, 2013, **42**, 9847; (*b*) M. Tenne, Y. Unger and T. Strassner, *Acta Crystallogr., Sect. C: Cryst. Struct. Commun.*, 2012, **68**, m203.

21 (*a*) T. Hofbeck and H. Yersin, *Inorg. Chem.*, 2010, **49**, 9290; (*b*) H. Wiedenhofer, S. Schuetzenmeier, A. von Zelewsky and H. Yersin, *J. Phys. Chem.*, 1995, **99**, 13385.

22 Y. Zhang, J. Clavadetscher, M. Bachmann, O. Blacque and K. Venkatesan, *Inorg. Chem.*, 2014, **53**, 756.

23 Y. Zhang, O. Blacque and K. Venkatesan, *Chem.–Eur. J.*, 2013, **19**, 15689.

24 F. May, M. Al-Helwi, B. Baumeier, W. Kowalsky, E. Fuchs, C. Lennartz and D. Andrienko, *J. Am. Chem. Soc.*, 2012, **134**, 13818.

25 (*a*) K. M.-C. Wong and V. W.-W. Yam, *Acc. Chem. Res.*, 2011, **44**, 424; (*b*) X. Yang, C. Yao and G. Zhou, *Platinum Met. Rev.*, 2013, **57**, 2.

26 H. Li, J. Li, J. Ding, W. Yuan, Z. Zhang, L. Zou, X. Wang, H. Zhan, Z. Xie, Y. Cheng and L. Wang, *Inorg. Chem.*, 2014, **53**, 810.

27 G. S.-M. Tong and C.-M. Che, *Chem.–Eur. J.*, 2009, **15**, 7225.

28 A. Tronnier, A. Poethig, E. Herdtweck and T. Strassner, *Organometallics*, 2014, **33**, 898.

29 G. L. Petretto, M. Wang, A. Zucca and J. P. Rourke, *Dalton Trans.*, 2010, **39**, 7822.

30 A. Vlcek and S. Zalis, *Coord. Chem. Rev.*, 2007, **251**, 258.

31 Y. Unger, T. Strassner and C. Lennartz, *J. Organomet. Chem.*, 2013, **748**, 63.

32 D. Drew and J. R. Doyle, *Inorg. Synth.*, 1990, **28**, 346.

33 C. Zhang, P. Yang, Y. Yang, X. Huang, X.-J. Yang and B. Wu, *Synth. Commun.*, 2008, **38**, 2349.

34 Y.-Z. Huang, H. Miao, Q.-H. Zhang, C. Chen and J. Xu, *Catal. Lett.*, 2008, **122**, 344.

35 M. J. Frisch, G. W. Trucks, H. B. Schlegel, G. E. Scuseria, M. A. Robb, J. R. Cheeseman, G. Scalmani, V. Barone, B. Mennucci, G. A. Petersson, H. Nakatsuji, M. Caricato, X. Li, H. P. Hratchian, A. F. Izmaylov, J. Bloino, G. Zheng, J. L. Sonnenberg, M. Hada, M. Ehara, K. Toyota, R. Fukuda, J. Hasegawa, M. Ishida, T. Nakajima, Y. Honda, O. Kitao, H. Nakai, T. Vreven, J. A. Montgomery Jr, J. E. Peralta, F. Ogliaro, M. Bearpark, J. J. Heyd, E. Brothers, K. N. Kudin, V. N. Staroverov, R. Kobayashi, J. Normand, K. Raghavachari, A. Rendell, J. C. Burant, S. S. Iyengar, J. Tomasi, M. Cossi, N. Rega, J. M. Millam, M. Klene, J. E. Knox, J. B. Cross, V. Bakken, C. Adamo, J. Jaramillo, R. Gomperts, R. E. Stratmann, O. Yazyev, A. J. Austin, R. Cammi, C. Pomelli, J. W. Ochterski, R. L. Martin, K. Morokuma, V. G. Zakrzewski, G. A. Voth, P. Salvador, J. J. Dannenberg, S. Dapprich, A. D. Daniels, Ö. Farkas, J. B. Foresman, J. V. Ortiz, J. Cioslowski and D. J. Fox, Gaussian, Inc., Wallingford CT, Gaussian 09, Rev. B 0.1, 2009.

36 (*a*) A. D. Becke, *J. Chem. Phys.*, 1993, **98**, 5648; (*b*) C. Lee, W. Yang and R. G. Parr, *Phys. Rev. B: Condens. Matter Mater. Phys.*, 1988, **37**, 785; (*c*) B. Miehlich, A. Savin, H. Stoll and H. Preuss, *Chem. Phys. Lett.*, 1989, **157**, 200; (*d*) S. H. Vosko, L. Wilk and M. Nusair, *Can. J. Phys.*, 1980, **58**, 1200; (*e*) P. J. Stephens, F. J. Devlin, C. F. Chabalowski and M. J. Frisch, *J. Phys. Chem.*, 1994, **98**, 11623.

37 (*a*) A. D. Becke, *Phys. Rev. A*, 1988, **38**, 3098; (*b*) J. P. Perdew, *Phys. Rev. B: Condens. Matter Mater. Phys.*, 1986, **33**, 8822; (*c*) J. P. Perdew, *Phys. Rev. B: Condens. Matter Mater. Phys.*, 1986, **34**, 7406.

38 (*a*) R. Ditchfield, W. J. Hehre and J. A. Pople, *J. Chem. Phys.*, 1971, **54**, 724; (*b*) W. J. Hehre, R. Ditchfield and J. A. Pople, *J. Chem. Phys.*, 1972, **56**, 2257; (*c*) P. C. Hariharan and J. A. Pople, *Chem. Phys. Lett.*, 1972, **16**, 217; (*d*) P. C. Hariharan and J. A. Pople, *Theor. Chim. Acta*, 1973, **28**, 213; (*e*) P. C. Hariharan and J. A. Pople, *Mol. Phys.*, 1974, **27**, 209; (*f*) V. A. Rassolov, J. A. Pople, M. A. Ratner and T. L. Windus, *J. Chem. Phys.*, 1998, **109**, 1223; (*g*) V. A. Rassolov, M. A. Ratner, J. A. Pople, P. C. Redfern and L. A. Curtiss, *J. Comput. Chem.*, 2001, **22**, 976.

39 (*a*) P. J. Hay and W. R. Wadt, *J. Chem. Phys.*, 1985, **82**, 299; (*b*) P. J. Hay and W. R. Wadt, *J. Chem. Phys.*, 1985, **82**, 270; (*c*) W. R. Wadt and P. J. Hay, *J. Chem. Phys.*, 1985, **82**, 284.

40 R. Dennington II, T. Keith, J. Millam, K. Eppinnett, W. L. Hovell and R. Gilliland, Semichem Inc.: Shawnee Mission, GaussView, 3.09, 2003.

41 C. Y. Legault, Université de Sherbrooke, CYLview, 1.0b, 2009.

42 G. M. Sheldrick, University of Goettingen, Goettingen, Germany,SADABS, Version 2.10, 2002.

43 (*a*) A. Altomare, G. Cascarano, C. Giacovazzo, A. Guagliardi, M. C. Burla, G. Polidori and M. Camalli, *J. Appl. Crystallogr.*, 1994, **27**, 435; (*b*) A. Altomare, M. C. Burla, M. Camalli, G. L. Cascarano, C. Giacovazzo, A. Guagliardi, A. G. G. Moliterni, G. Polidori and R. Spagna, *J. Appl. Crystallogr.*, 1999, **32**, 115.

44 G. M. Sheldrick, *Acta Crystallogr., Sect. A: Found. Crystallogr.*, 2008, **64**, 112.

45 A. J. C. Wilson and Editor, Mathematical, Physical and Chemical Tables, *International Tables for Crystallography*, Kluwer, 1992, vol. C.

46 R. W. W. Hooft and B. V. Nonius, *Data Collection Software for Nonius-Kappa CCD*, Delft, The Netherlands, 1999.

47 A. J. M. Duisenberg, *J. Appl. Crystallogr.*, 1992, **25**, 92.

48 A. J. M. Duisenberg, L. M. J. Kroon-Batenburg and A. M. M. Schreurs, *J. Appl. Crystallogr.*, 2003, **36**, 220.

49 A. L. Spek, *Acta Crystallogr., Sect. D: Biol. Crystallogr.*, 2009, **65**, 148.

50 G. M. Sheldrick, *Program for the Refinement of Structures*, University of Goettingen, Goettingen, Germany, SHELXL-97, 1997.
51 C. F. Macrae, I. J. Bruno, J. A. Chisholm, P. R. Edgington, P. McCabe, E. Pidcock, L. Rodriguez-Monge, R. Taylor, J. van de Streek and P. A. Wood, *J. Appl. Crystallogr.*, 2008, **41**, 466.
52 (*a*) M. N. Burnett and C. K. Johnson, Oak Ridge National Laboratory, Oak Ridge, TN, USA, ORTEP-III, 2000; (*b*) L. J. Farrugia, *J. Appl. Crystallogr.*, 1997, **30**, 565.